Hindawi Publishing Corporation
Journal of Biomedicine and Biotechnology
Volume 2010, Article ID 167045, 10 pages
doi:10.1155/2010/167045

Research Article

Identification of a New Peptide for Fibrosarcoma Tumor Targeting and Imaging In Vivo

Chia-Che Wu,[1,2] Erh-Hsuan Lin,[3,4] Yu-Ching Lee,[5] Cheng-Jeng Tai,[6] Tsu-Hsiang Kuo,[3,7] Hsin-Ell Wang,[8] Tsai-Yueh Luo,[9] Ying-Kai Fu,[9] Haw-Jan Chen,[9] Ming-Ding Sun,[3] Chih-Hsiung Wu,[10] Cheng-Wen WU,[4] Sy-Jye Leu,[11] and Win-Ping Deng[3]

[1]*Graduate Institute of Clinical Medicine, Taipei Medical University, Taipei 11031, Taiwan*
[2]*Department of Otolaryngology, Wan-Fang Hospital, Taipei Medical University, Taipei 116, Taiwan*
[3]*Institute of Biomedical Materials and Engineering, Taipei Medical University, 250 Wu-Hsing Street, Taipei 110, Taiwan*
[4]*Institute of Biochemistry and Molecular Biology, National Yang-Ming University, Taipei 112, Taiwan*
[5]*Genomics research Center, Academia Sinica, Taipei 115, Taiwan*
[6]*Section of Hematology-Oncology, Department of Medicine, Taipei Medical University, Taipei 11217, Taiwan*
[7]*Graduate Institute of Life Sciences, National Defense Medical Center, Taipei 114, Taiwan*
[8]*Institute of Radiological Science, National Yang-Ming University, Taipei 112, Taiwan*
[9]*Institute of Nuclear Energy Research, Taoyuan 32546, Taiwan*
[10]*Department of Surgery, School of Medicine, Taipei Medical University-Shuang Ho Hospital, Taipei 110, Taiwan*
[11]*Department of Microbiology and Immunology, School of Medicine, Taipei Medical University, 250 Wu-Hsing Street, Taipei 110, Taiwan*

Correspondence should be addressed to Sy-Jye Leu, cmbsycl@tmu.edu.tw and Win-Ping Deng, wpdeng@ms41.hinet.net

Received 14 April 2010; Revised 9 August 2010; Accepted 2 October 2010

Academic Editor: Elvira Gonzalez De Mejia

A 12-mer amino acid peptide SATTHYRLQAAN, denominated TK4, was isolated from a phage-display library with fibrosarcoma tumor-binding activity. In vivo biodistribution analysis of TK4-displaying phage showed a significant increased phage titer in implanted tumor up to 10-fold in comparison with normal tissues after systemic administration in mouse. Competition assay confirmed that the binding of TK4-phage to tumor cells depends on the TK4 peptide. Intravenous injection of ^{131}I-labeled synthetic TK4 peptide in mice showed a tumor retention of 3.3% and 2.7% ID/g at 1- and 4-hour postinjection, respectively. Tumor-to-muscle ratio was 1.1, 5.7, and 3.2 at 1-, 4-, and 24-hour, respectively, and tumors were imaged on a digital γ-camera at 4-hour postinjection. The present data suggest that TK4 holds promise as a lead structure for tumor targeting, and it could be further applied in the development of diagnostic or therapeutic agent.

1. Introduction

Metastasis to the lung is often a lethal cause in sarcomas and other cancers [1, 2]. Many attempts to eradicate cancer through conventional therapy (irradiation or chemotherapy) are ineffective, mainly because of treatment resistance [3–5]. Highly metastatic cells tend to exhibit a greater survival ability and resistance to apoptosis than poorly metastatic ones. New imaging procedures for diagnosis, treatment planning, and therapy of metastatic cancer are thus required for accurate staging. Several attempts to optimize the methods for imaging lung metastases have been described, such as bioluminescence imaging (BLI) or fluorescence reflectance imaging (FRI) of HT-1080 fibrosarcoma cells labeled with luciferase or green fluorescent protein (GFP), respectively [6, 7], and single photon emission computed tomography (SPECT) of prostate cancer cells expressing Na+/I-symporter [8], or fibrosarcoma cells expressing herpes simplex virus type 1 thymidine kinase (HSV1-tk) [9]. However, although these models have great potential in preclinical researches, the need of the stable expression of an exogenous marker gene limited their applications in clinic. Efficient molecular

tracers that can target metastatic tumors through binding an endogenous receptor expressing on cancer cells need to be developed.

Peptides are promising molecules to selectively deliver imaging or therapeutic agents to tumors. Peptides have several advantages such as small size, good tissue diffusion, target accessibility, no antigenicity, easy synthesis, and adequate radiolabeling [10]. The application of a specific tumor-targeting peptide requires enough binding sites (e.g., an overexpressed cell surface receptor), high affinity of the ligand, and sufficient in vivo stability [11]. Some peptide probes such as somatostatin, gastrin, bombesin, GLP-1, and RGD analog peptides have been extensively examined and applied to diagnosis and radiopeptide therapy [10]. Most of these peptides target tumor by recognizing a regulator peptide receptor overexpressed in tumors. For example, somatostatin analogs, the most prominent example of tumor-specific peptide, recognize mainly somatostatin receptor subtype 2 overexpressed in neuroendocrine tumors [12]. Bombesin (also known as gastrin-releasing peptide (GRP)) analogs were applied in diagnostic imaging of prostate and breast tumors in clinic [13, 14]. RGD motif does not belong to the regulatory peptide family, but is present in extracellular matrix (ECM) components like fibrinogen and vitronectin, which interact with integrin receptors on cells [15]. RGD-based peptides were developed to target neoangiogenic endothelial and various types of tumors in preclinical models [16].

The identification of new tracer peptides that can target tumor cells with sufficient specificity and reduced background binding for in vivo imaging remains a challenge. Phage display is a powerful technique to identify novel short peptides that can bind to proteins or other macromolecules, with the major advantage of rapidly selecting a target-specific peptide from a vast DNA library [17]. Phage display technique has also been used to discover numerous novel peptides with specificity to various types of cancer, and some have been further applied in drug delivery and diagnosis researches (for a recent review, see [18]).

Our lab has previously reported the use of planar γ-camera for noninvasive imaging of tumor progression and gene therapy in an experimental blood-borne lung metastases model using fibrosarcoma cells expressing HSV1-tk [9]. Nevertheless, the imaging relied on the expression of an exogenous reporter gene integrated in tumor cells. In the current research, we intend to develop a peptide tracer that can target fibrosarcoma tumors in vivo without the need of an exogenous marker in tumor cells. A novel peptide was selected through phage-display biopanning. Biodistribution analysis and noninvasive imaging using planar γ-camera showed efficient homing and accumulation of the peptide in tumor site in mice. The peptide shows no sequence similarity to other peptides currently known for tumor imaging, but is homologous to a sequence present in the sixth fibronectin type III domain of a novel protein similar to vertebrate fibronectin type III domain-containing protein family (GenBank: CAQ14006.1). The binding of this peptide to cancer cells was inhibited by fibronectin, suggesting that it may have targeted cells through fibronectin-interacting site(s). These results recommend the novel peptide as a promising lead structure for tumor-targeting agent.

2. Material and Method

2.1. Cell Culture. The NG4TL4-tk cell line was constructed from the parental NG4TL4 fibrosarcoma cell line [19] (China Medical University, Taiwan) by transfecting with packaged virions of a bicistronic retroviral vector containing HSV1-tk gene [9]. NG4TL4-tk cells were cultured in minimum essential medium (MEM) supplemented with 10% fetal bovine serum (FBS), 100 units/mL penicillin, 10 mg/mL streptomycin, and 2 mM L-glutamine (all from Gibco Invitrogen Ltd., Taiwan) in humidified atmosphere with 5% CO_2 at 37°C.

2.2. Animal and Tumor Implantation. Female 6-week-old FVB/N mice were obtained from National Taiwan University Laboratory Animal Center. NG4TL4-tk cells (5×10^5) resuspended in 200 μl of PBS were injected subcutaneously into the right limb of the mouse to form tumor. All animal experiment protocols were approved by the Institutional Animal Care and Use Committee of Taipei Medical University.

2.3. Phage Display and Panning Process. The 12-mer peptide library (Ph.D.12, New England Biolabs, MA, USA) was used for panning process. Briefly, 10^6 cancer cells were collected and fixed with ice-cold glutaraldehyde (0.125% in PBS) for 10 minutes, washed with PBS, blocked with 3% (w/v) BSA in PBS, and then incubated with $\sim 10^{12}$ phage clones for 1 hour at room temperature (RT). After extensive washes with PBS, cells were collected by centrifuge, and the bound phages were eluted with 200 μl of elution buffer (20 mM Glycine-HCl, pH 2.2) and then neutralized by adding 12 μl of neutralization buffer (2 M Tris-HCl, pH 9.1). The eluted phages were amplified in ER2738 bacteria according to the manufacturer's protocol and used for the next round of panning. Four rounds of panning were performed. The phages selected after the final round were amplified and stored. To identify the DNA sequence of the peptide displayed on the phage, single-phage plaques were picked up and amplified for sequencing using a primer corresponding to phage pIII gene sequence: 5′-CCCTCATAGTTAGCGTAACG-3′.

2.4. In Vitro and In Vivo Phage-Binding Assay. For in vitro phage-binding assay, 10^6 cancer cells in suspension were mixed with 5×10^{10} testing phages in PBS for 2 h at 37°C. After 5 washes with PBS, bound phages were eluted and neutralized as described. Recovered phages were amplified in ER2738 bacteria and the titer was determined by standard plaque-forming analysis. For immunofluorescent microscopic examination, cells were seeded on glass coverslips by 10^5 cells/well in a 24-well plate overnight. The following day, cells were incubated with 5×10^{10} pfu of phages for 1 hour at RT. After 5 washes with PBS, cells were fixed in 2% formaldehyde and blocked with PBS containing 10%

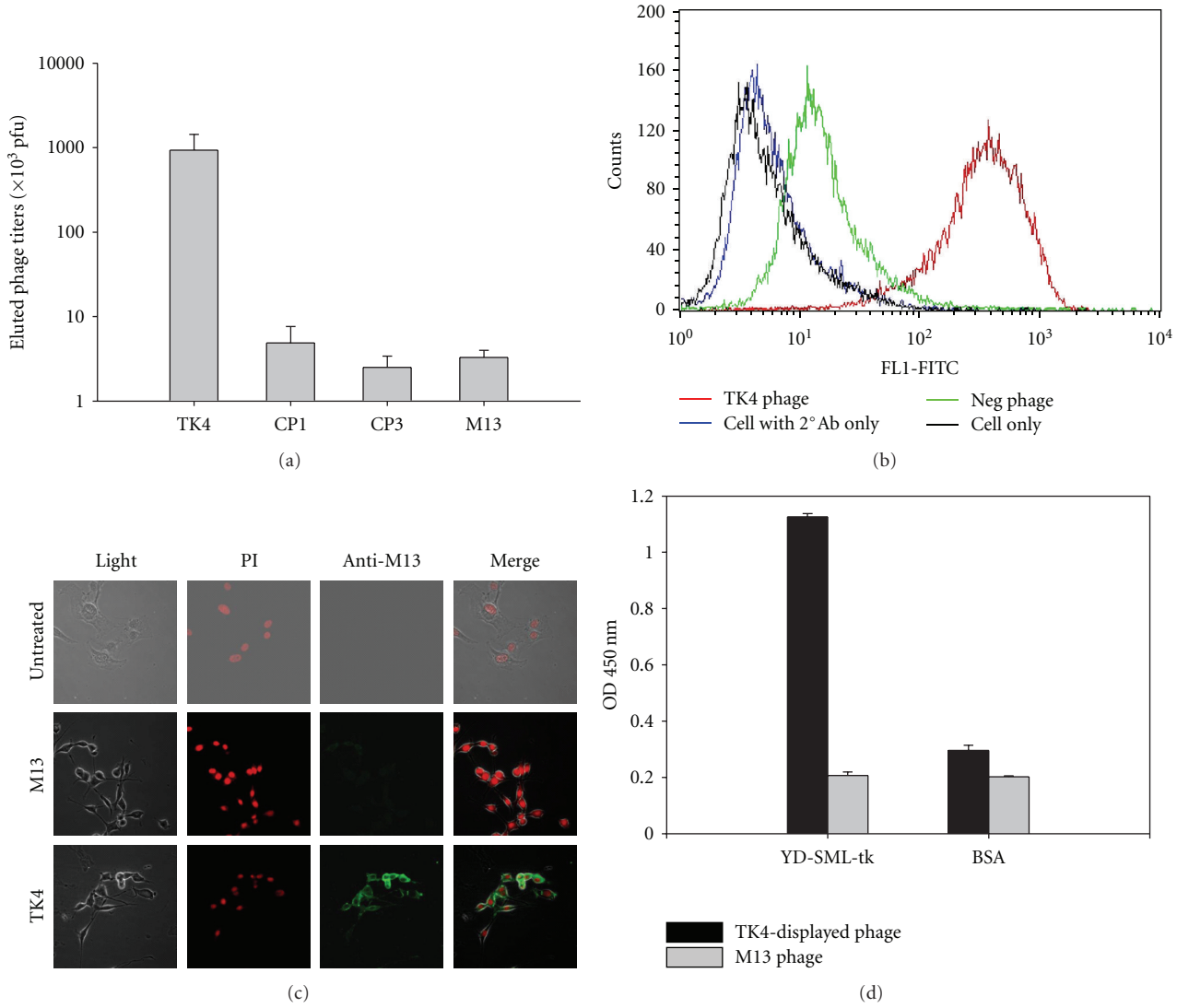

FIGURE 1: In vitro binding assay of TK4-phage to NG4TL4-tk tumor cells. (a) NG4TL4-tk cells were incubated with the indicated phages for affinity examination. After extensive washing, bound phages were eluted from cells and titered as pfu. CP1 and CP3 are phages displaying irreverent peptide. M13 is the wild-type phage. (b) Binding of TK4-expressing phage to NG4TL4-tk cells was verified by flow cytometry with an anti-M13 antibody. Untreated cells (cell only), cells treated with 2nd antibodies only, and cells reacted with the wild-type M13 phages (neg phage) served as negative controls. (c) NG4TL4-tk cells were incubated with 5×10^{10} pfu of TK4 or wild-type (M13) phages. Bound phages were detected using a primary anti-M13 antibody and a FITC-conjugated secondary antibody (green) and were investigated by a fluorescence-activated laser scanning microscope. Nuclei were counterstained with PI solution (red). Wild-type phage and untreated cell served as controls. (d) TK4-displaying phages (10^7 pfu) were incubated with NG4TL4-tk cell lysate coated in microtiter wells. After washes, the bound phages were detected using an HRP-conjugated anti-M13 antibody and measured at OD 450 nm. BSA and wild-type M13 phage served as control antigen and phage, respectively.

FBS. Cells were incubated with the primary mouse anti-M13 antibody (1 : 3000) and then with the secondary FITC-conjugated antimouse antibody (1 : 3000), for 1 hr at 37°C, respectively. Nuclei were counterstained with Propidium Iodide (PI) (1 μg/ml), and the slide was subjected to a fluorescence-activated laser scanning microscope (TCS SP5 Confocal Spectral Microscope, Leica, USA). Wild-type phage M13 and an untreated sample served as controls.

For in vivo biodistribution analysis, 200 μl of PBS containing 10^{12} phages with or without the competitive synthetic TK4 peptide were injected IV into the tumor-bearing mice through tail vein. Five minutes after injection, mice were perfused through heart with 50 ml of PBS. Tumor and normal organs including kidney, liver, lung, and heart were removed. After homogenization, 100 μg of each tissue was washed with PBST for 3 times and incubated in 200 μl of elution buffer at RT with gently shaking for 10 minutes. Recovered phages were neutralized and titered by plaque-forming assay and normalized as pfu per gram of tissue.

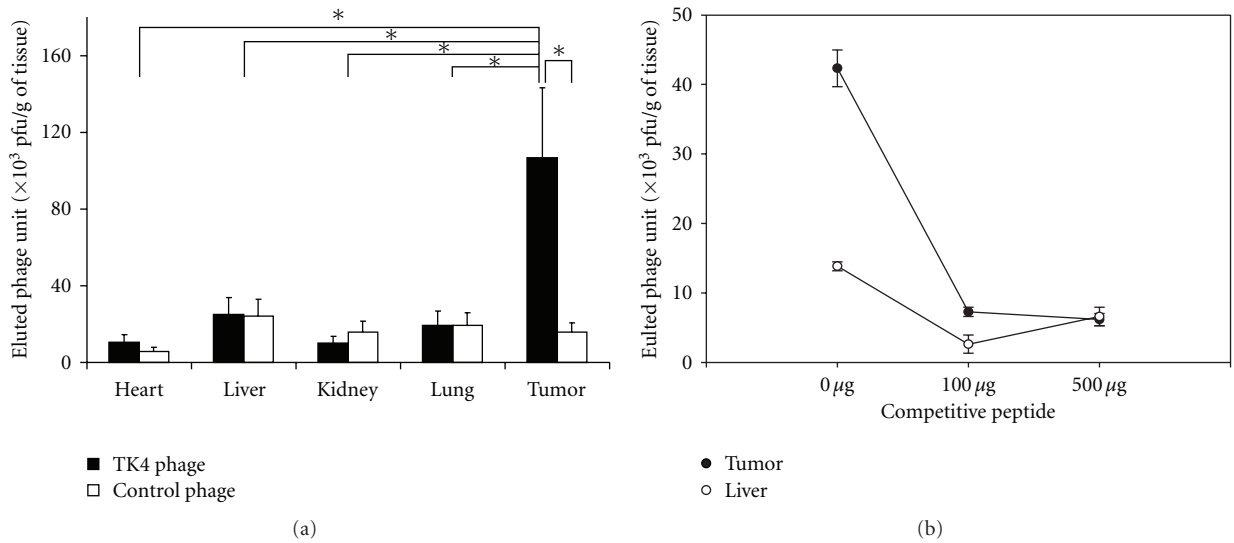

Figure 2: Biodistribution of TK4-displaying phage in vivo. (a) TK4-displaying or CP1 control phage (10^{12}) was dissolved in PBS (200 μl) and IV injected into the tumor-bearing mice. The titers of phage (pfu/g of tissue) recovered from tumor and other tissues were averaged from duplications of 3 mice. Error bar represents the Standard Error of Mean (SEM). *P*-values were calculated by Student's *t*-Test with two-tails (*, $P < .05$). (b) TK4-displaying phages were injected into mice in the presence of different amount (0 to 500 μg) of the competitive synthetic TK4 peptide. The phages were eluted form tumor and liver homogenates and titered as pfu.

2.5. Phage ELISA. Cancer cells were broken by sonication. After centrifuge, the supernatant was collected and measured for protein concentration using Protein Assay kit (Bio-Rad, USA) and then diluted in the coating buffer (0.1 M $NaHCO_3$, pH 8.6). Microtiter wells (Coster, USA) were coated with 0.5 μg/well of cell lysate or BSA in coating buffer at 4°C overnight and then blocked with 3% (w/v) BSA in PBST at 37°C for 1 hr. 10^7 of testing phage was added to the wells and incubated at RT for 2 hours. After 5 washes with PBST, 50 μl of diluted (1 : 1000) HRP-conjugated anti-M13 antibody (GE Healthcare Bio-Sciences, NJ, USA) was added to each well and incubated at RT for 1 hour. After 5 washes with PBST, each well was incubated with 50 μl of TMB substrate solution (KPL, MD, USA) in the dark for 30 minutes of development at RT. The reaction was stopped by adding 1 N HCl (25 μl/well), and the plate was read using a microplate reader at 450 nm.

2.6. Flow Cytometry Analysis. Cancer cells (10^6) were collected and fixed with 2% formaldehyde and blocked with 1% (w/v) BSA in PBS. Testing phages (5×10^{10} pfu) were incubated with cells for 2 hour at 37°C, followed by 5 washes with PBS. The bound phages were labeled by incubating with a primary mouse anti-M13 antibody (1 : 3000) (GE Healthcare Bio-Sciences, NJ, USA) for 1 hr at 37°C and then with a secondary fluorescein isothiocyanate (FITC) conjugated antimouse antibody (1 : 3000) (Sigma-Aldrich, USA) for 1 h at 37°C. The fluorescent signal of each cell was analyzed by FACScan flow cytometry (Becton Dickinson, NJ, USA).

2.7. Peptide and In Vitro Binding Assay. The synthetic 12-mer amino acid peptide TK4 (SATTHYRLQAAN) was purchased from Kelowna International Scientific Inc. (Taipei, Taiwan), with FITC conjugated on the N-terminal (FITC-TK4). For in vitro binding assay, cells were seeded on coverslips in 24-well plate by 10^5 cells/well. The following day, cells were washed by PBS and incubated in serum-free medium containing fibronectin (Sigma-Aldrich, USA) in a concentration 0, 2, or 20 μg/ml for 30 min at 37°C. Mediums were then removed, cells were washed by PBS and then incubated in serum-free medium containing FITC-TK4 (40 μM) for 1 hr at 37°C. Medium was removed, and cells were washed 3 times in PBS for 5 min. Cells were fixed in 4% PFA for 10 min at RT and then mounted on slides by mounting medium containing DAPI (Vector Lab, CA, USA) and examined on a fluorescent microscope (BX41, Olympus, Japan).

2.8. In Vivo Imaging and Biodistribution Analysis of TK4 Peptide. For biodistribution analysis and in vivo imaging, synthetic FITC-TK4 was further labeled on the benzene group of FITC with isotopic ^{131}I ([^{131}I]-FITC-TK4). The [^{131}I]-FITC-TK4 used in animal experiment was solved in PBS at a concentration of 50 μg/100 μCi/100 μl. Mice were pretreated with 0.5 mL of 0.9% NaI (w/v) solution by intraperitoneal injection 15 min before [^{131}I]-FITC-TK4 administration to diminish thyroid uptake of the liberated ^{131}I coming from [^{131}I]-FITC-TK4. Each mouse was then IV injected with 50 μg of [^{131}I]-FITC-TK4 (100 μCi) dissolved in 100 μl of PBS. The planar γ-camera imaging was performed as described [9]. Briefly, static images were obtained from anesthetized animals at 1, 4, and 24 hr with a digital γ-camera (Elscint SP-6, Haifa, Israel), equipped with a high-energy pinhole collimator, a 364-keV 6 10% ^{131}I photopeak energy window, and a $256 \times 256 \times 16$ bit image matrix. The mice injected with ^{131}I (100 μCi) solution served as

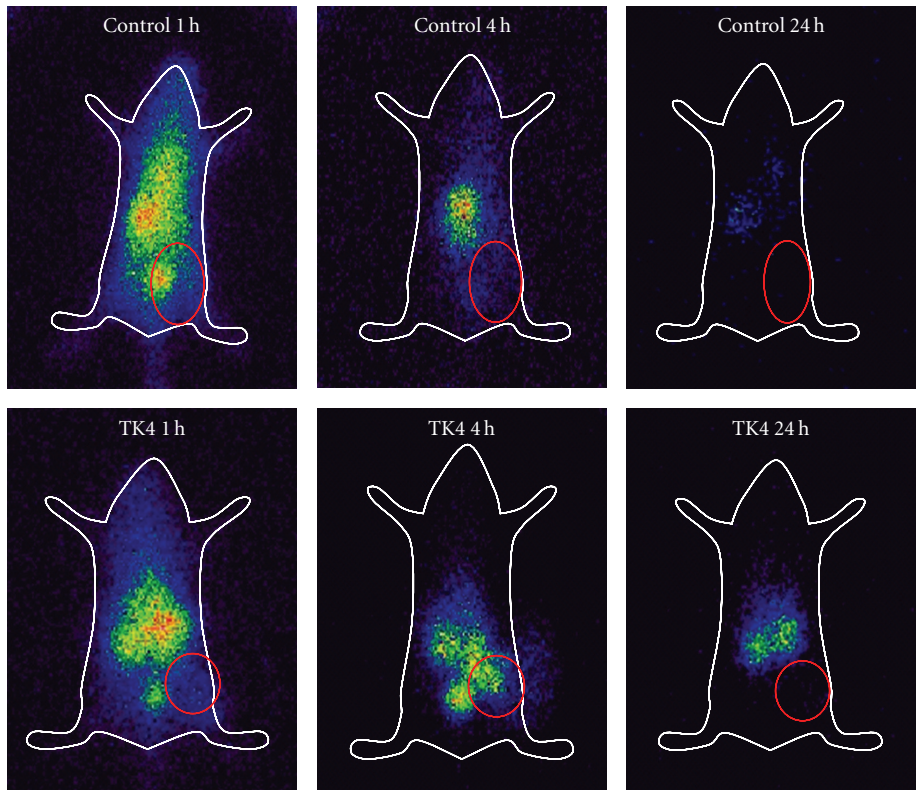

(a)

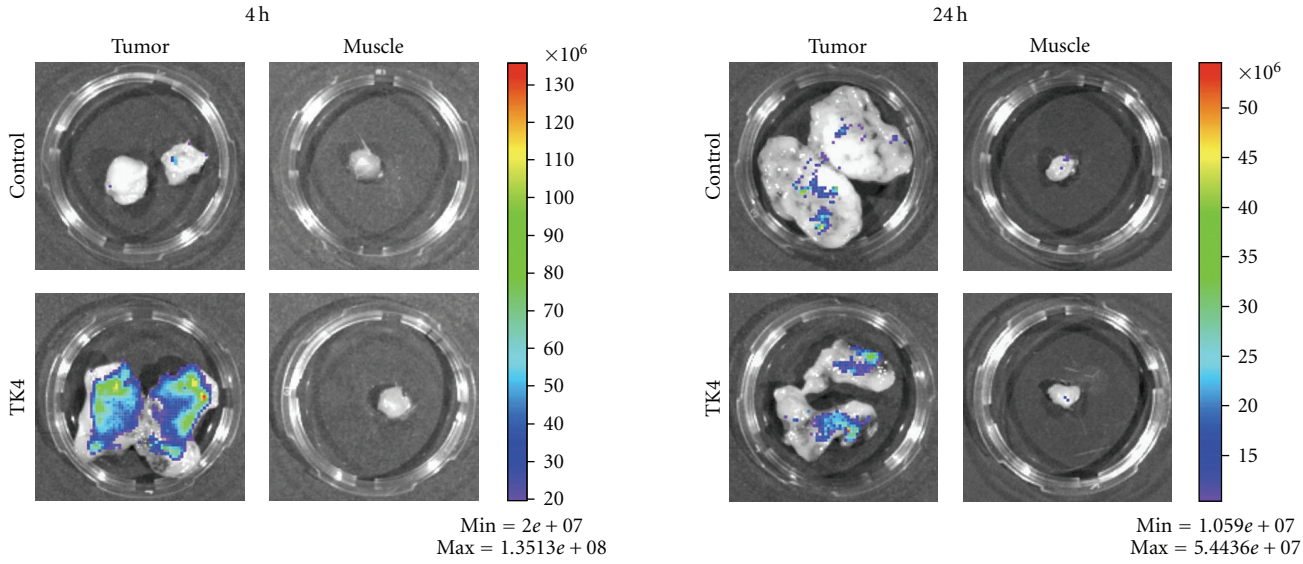

(b)

Figure 3: TK4 peptide-based tumor imaging in vivo. (a) Mice were injected with 50 μg (100 μCi) of [^{131}I]-FITC-TK4 through tail vein and imaged at indicated time points on (a). Red circles indicate the location of tumor. The injection of ^{131}I (100 μCi) served as negative control. (b) Mice were injected with [^{131}I]-FITC-TK4 as described and sacrificed at 4 or 24 hr, from which tumors and muscles were removed, dissected, and imaged using IVIS 200 optical system to detect of FITC signal inside tumor. The injection of ^{131}I (100 μCi) served as negative control.

Table 1: Peptide sequences expressed on phage clones binding to NG4TL4-tk.

Amino acid sequence	Number of hit
*SATTHYRLQAAN	11
TEHPSNTSPMRL	2
SGNTHYRLQAAN	1
TPHRLDWSPHLV	1

* Denominated "TK4" in this report.

negative control. For biodistribution analysis, mice were sacrificed at indicated time points after injection. Tumors and organs were removed and weighed, and the radioactivity was determined using a γ-counter. Results were calculated as the percentage of injected dose per gram (% ID/g) of tissue. Tumors removed from sacrificed mice were also dissected and imaged using IVIS-200 optical system (Xenogen, CA, USA) for the detection of FITC signal. Data were analyzed by Living Image software version 2.50 (Xenogen).

3. Result

3.1. Selection of the Peptide Binding to Fibrosarcoma Cells. For the selection of a peptide with specific binding affinity to fibrosarcoma cell line NG4TL4-tk, a phage library expressing variant surface 12-mer peptides was used for in vitro biopanning. For each round, 10^{12} phages were incubated with 10^6 cancer cells for 1 hr and the unbound phages were washed off. The bound phages were then eluted from cancer cells and amplified in bacteria for the next round of panning. After 4 panning rounds, single-phage clones were selected and amplified, and the phage DNA was sequenced. Among 15 clones sequenced, 11 ones (73%) showed the same peptide sequence: SATTHYRLQAAN (named TK4 in the following text) (Table 1). The phage expressing TK4 as well as the synthetic TK4 peptide were used for further evaluation.

3.2. Specific Binding of TK4-Displaying Phage to Fibrosarcoma Cells In Vitro and In Vivo. The TK4-displaying phage (TK4-phage) was analyzed for the binding affinity to NG4TL4-tk fibrosarcoma cells. Tumor cells were incubated with selected phages. After extensive washes, the bound phages were eluted from cells and titered by a standard plaque-forming assay. The results showed that only the phage clone displaying TK4 peptide was substantially eluted from NG4TL4-tk cells (Figure 1(a)). The binding of TK4-phage to NG4TL4-tk cells was further confirmed by flow cytometry analysis using an anti-M13 antibody (Figure 1(b)). Immunofluorescent (IF) microscopic examination with the same anti-M13 antibody detected the attachment of TK4-phage, but not the wild-type phage, on the surface of NG4TL4-tk cells (Figure 1(c)). To confirm that the binding affinity of TK4-phages to cell did not result from the random absorption on cell membrane, tumor cells were lysed and coated on microtiter wells by 0.5 μg of protein per well. TK4- or wild-type phages were incubated with the lysate. After extensive washes, the phages retaining in the well were detected using an HRP-conjugated anti-M13 antibody and quantified by measuring OD 450 nm after substrate incubation. The result showed that TK4-phages adhered strongly to tumor lysate but not to control peptide, while the wild-type M13 phages adhered to neither (Figure 1(d)). In summary, these results showed that TK4-phage bound to NG4TL4-tk fibrosarcoma cells and suggested that the binding was associated with one (or more) specific cell-surface protein receptor(s).

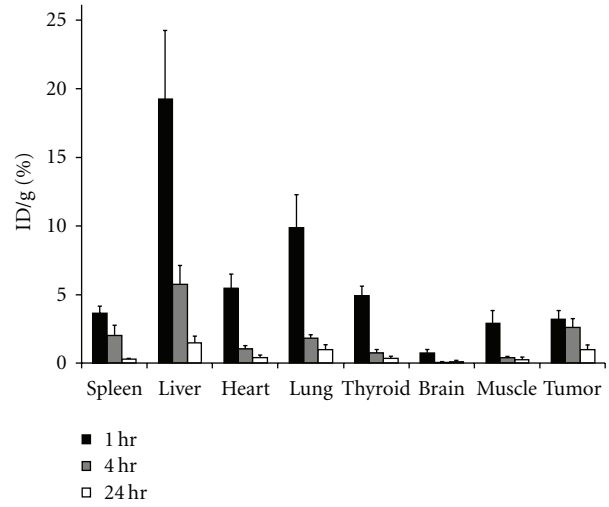

Figure 4: Biodistribution of TK4 in tumor-bearing mouse. Animals receiving IV injected ^{131}I-FITC-TK4 were sacrificed at 1, 4, or 24 hr postinjection. Tumors and other organs were removed and measured for the radioactivity. Results were calculated as percentage of injected dose per gram of tissue (% ID/g). Error bars indicate SEM. $N = 5$ at each time point.

To investigate the tumor targeting of TK4-phage in vivo, phages were injected into tumor-bearing mice intravenously (IV) through tail vein. Five minutes after injection, mice were sacrificed and perfused. Phages were recovered from the homogenates of removed tumor or other organs and were titered by a standard plaque-forming assay. The result showed a significant increase of TK4-phage titer in implanted tumor up to 10-fold in comparison with other organs (Figure 2(a)). In contrast, CP1 control phage did not show any preferential targeting. To confirm that the tumor homing of TK4-phage is dependent on the displayed TK4 peptide, the phage was premixed with synthetic TK4 peptide before injection. The TK4-phage titers eluted from tumors reduced dramatically after incubation with 100 μg of TK4 peptide (Figure 2(b)). These results showed that TK4-phage performed the in vivo tumor-homing ability, which was dependent on the displayed TK4 peptide.

3.3. TK4 Peptide-Based Tumor Imaging and Biodistribution. To examine the availability of TK4 peptide as an in vivo tumor-imaging probe, the synthetic TK4 peptide was labeled with FITC and isotopic ^{131}I ([^{131}I]-FITC-TK4), and IV injected to mice through tail vein. To diminish the thyroid accumulation of liberated ^{131}I, mice were pretreated with 0.9% NaI solution intraperitoneally. Whole-body images

Table 2: Tumor-to-tissue ratios of % ID/g calculated from the biodistribution of [^{131}I]-TK4 at different time points.

Tumor-to-organ ratio	1 hr	4 hr	24 hr
Intestine	0.20	0.22	1.25
Spleen	0.89	1.28	2.96
Liver	0.17	0.46	0.67
Kidney	0.07	0.07	0.03
Heart	0.60	2.38	2.15
Lung	0.33	1.39	0.98
Thyroid	0.66	3.31	2.44
Brain	4.00	22.81	6.73
Muscle	1.10	5.73	3.15
Tumor	1.00	1.00	1.00

were taken on a planar γ-camera 1, 4, and 24 hrs postinjection. The results showed that at 4 hr, TK4 signal was detected in tumor site, which then diminished and became unrecognizable in 24 hrs (Figure 3(a)). Tumors were also removed from mice sacrificed at 4 or 24 hrs, dissected, and imaged for FITC signal using FRI (Figure 3(b)). The results confirmed a much stronger accumulation of TK4 peptide inside the tumor as compared to surrounding muscle. Biodistribution analysis of injected peptide was performed by measuring the radioactivity in tumor and other organs removed from sacrificed mice (Figure 4). The peptide uptake in tumor was $3.28 \pm 0.63\%$, $2.66 \pm 0.66\%$, and $1.03 \pm 0.76\%$ ID/g at 1, 4, and 24 hr postinjection, respectively. Although most organs showed higher or comparable radioactivities comparing to tumor at 1 hr, most of them reduced rapidly at 4 hr, while tumor retained most signal (>80%) (Figure 4). This would suggest that most radioactivity present in normal tissues resulted from unspecific accumulation. The uptake of TK4 was higher in tumor than in other organs at 4 hr except kidney, liver, and intestine (Table 2). Kidney and intestine exhibited considerable retention of radioactivity: $36.82 \pm 4.31\%$ and $12.02 \pm 5.45\%$ at 4 hr, respectively, suggesting that the [^{131}I]-FITC-TK4 was eliminated through both hepatobiliary and renal eliminations. The % ID/g ratio of tumor-to-muscle was 5.73 and 3.15 at 4 and 24 hr, respectively. Mice injected with ^{131}I (100 μCi) served as negative control, which showed no specific accumulation in γ-camera images or biodistribution analysis (Figure 3, data not shown).

3.4. Inhibitory Effect of Fibronectin on TK4 Binding. To understand whether TK4 shows sequence similarity to other peptides currently known for tumor targeting, we have searched in different protein databases, and the results showed no such similarity. Instead, the alignment using Protein Blast in NCBI found a high similarity between TK4 and a novel protein similar to vertebrate fibronectin type III domain-containing protein family (GenBank: CAQ14006.1) found in *Danio rerio* (zebrafish). The TK4 homologous sequence locates at the sixth fibronectin type III domain (FN3) of the protein (Figure 5(a)). Fibronectin is one of the major fractions of ECM that mediates interactions between cells, other ECM components (e.g., collagen) and other fibronectin molecules [15]. To test if TK4 could bind to fibronectin-interacting site(s), we performed an in vitro binding assay of TK4 on NG4TL4-tk cells. The results showed that TK4 binding was inhibited by pretreatment of cells with fibronectin in a dose-dependent manner (Figure 5(b)). These results implied a relationship between TK4 and fibronectin and would suggest that the binding of TK4 to cancer cells is associated with fibronectin-interacting components.

4. Discussion

Drug-resistant metastatic tumors as well as side effects are major limitations of conventional cancer therapy such as irradiation or chemotherapy [4, 5], which necessitate the search for novel tumor-targeting agents. Specific targeting of tumors, compared with earlier less specific approaches, is increasingly significant in oncology either for diagnostic or therapeutic purposes [10]. Our previous report has demonstrated the monitoring of tumor progression and gene therapy using noninvasive planar γ-camera imaging in a lung metastases model with murine fibrosarcoma cells, NG4TL4-tk, stably expressing HSV1-tk [9]. Following the previous work, in the current research, we are attempting to develop a new targeting agent which can label the same tumor cells in vivo without the need of the expression of an exogenous marker gene in tumor cells. Using the peptide phage display system on NG4TL4-tk cell line, a new tumor-binding peptide, TK4, was identified. TK4-phage was confirmed for the binding affinity to NG4TL4-tk cells in vitro with different methods including plaque-forming assay, flow cytometry, IF microscopy, and phage ELISA (Figure 1). IV administration of TK4-phage to mice bearing NG4TL4-tk tumors through tail vein showed significantly higher retention of phages in tumor than in other organs (Figure 2). As competitive synthetic TK4 peptide was premixed with TK4-phage, the phage titer eluted from tumors reduced to a level comparable to the control tissue. These results confirmed that TK4-phage maintained its tumor-targeting ability in vivo and that the binding is dependent on the displayed surface TK4 peptide.

These results recommended the potential of TK4 peptide as an in vivo tumor-targeting agent. Radio- and fluorescent-labeled TK4 ([^{131}I]-FITC-TK4) was thus synthesized and systemically administrated in tumor-bearing mice. Although a strong and unspecific distribution of TK4 signal was observed throughout the body 1 hr after injection, most signals diminished rapidly at 4 hr, while the tumor retained a comparable intensity, resulting in a high tumor-to-organ ratio (Figure 4 and Table 2). This observation would suggest that most signals accumulated in normal tissues were nonspecific. The uptake of TK4 was higher in tumor than in normal organs except kidney, liver, and intestine at 4 hr, and the tumor-to-muscle ratio of % ID/g was 5.73 (Table 2). The weak accumulation of radioactivity in collateral tissues made the diagnostic imaging of tumor more viable. The tumor site can be detected in a whole-body imaging using planar γ-camera at 4 hr postinjection (Figure 3(a)), and the

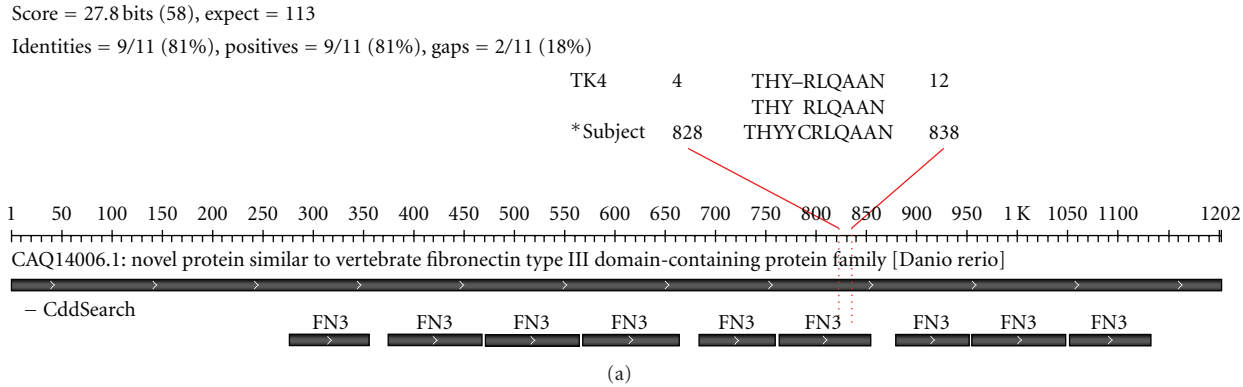

(a)

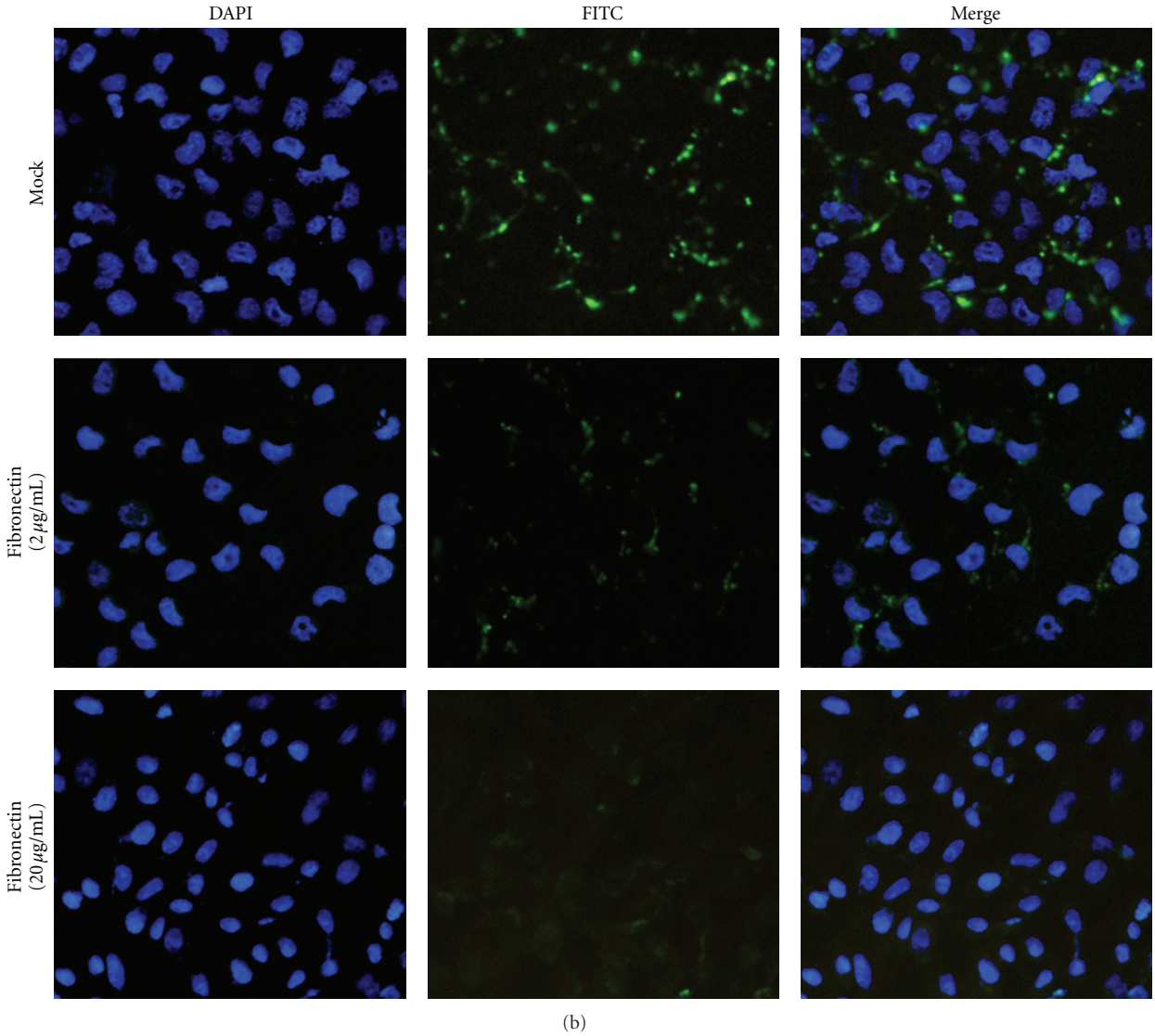

(b)

Figure 5: Inhibitory effect of fibronectin on TK4 binding. (a) *Subject: Novel protein similar to vertebrate fibronectin type III domain-containing protein family [Danio rerio], GenBank: CAQ14006.1. FN3: Fibronectin type III domain. The alignment result was obtained in Protein Blast of NCBI, and edited by NCBI Sequence Viewer (http://www.ncbi.nlm.nih.gov/projects/sviewer/). (b) NG4TL4-tk cells were pretreated with fibronectin in a concentrations of 0 (mock), 2, or 20 μg/ml (30 min, 37°C) before subjected to FITC-TK4 peptide (40 μM) incubation (1 hr, 37°C). Cells were extensively washed with PBS and then fixed in 4% PFA and mounted. Nuclei were counter stained by DAPI. Original magnification × 200.

FRI confirmed a much stronger FITC signal accumulated in tumors than in surrounding muscles (Figure 3(b)). All together, these results suggest that TK4 peptide is able to target and accumulate in fibrosarcoma tumors in vivo.

The difference in biodistributions between the phage particles and synthetic TK4 peptide was noticed (Figures 2 and 4). The phage particles showed an efficient binding only in tumor, while synthetic peptide had a high retention also in liver and kidney. Such discrepancy may have resulted from the different methodologies applied. Phage particles were recovered from tissues of sacrificed animal in a few minutes after administration, which may prevent the further accumulation of phages in excretion route like liver, intestine, or kidney. In addition, the whole body perfusion in sacrificed mice may have helped to wash off the unbound phages. To optimize the use of TK4 as an efficient tumor-imaging peptide; however, the substantial accumulation of radioactivity in kidney and liver should be reduced. Small changes in peptide sequence, linkers, chelator, and isotope can dramatically affect the biodistribution [18]. For example, a high radioactivity retention in liver and intestine could result from the hepatobiliary elimination. Strategies including glycosylation or conjugation with hydrophilic amino acid have been developed to reduce the liver uptake of RGD peptides (for a recent review, see [20]). Renal excretion is a preferable elimination pathway of radiopharmaceuticals and/or their metabolites from the body. Nevertheless, high kidney retention may obscure tumor imaging and result in potential radiation nephrotoxicity, and thus limit the use of radiolabelled peptides in medical applications [21, 22]. Current methods for kidney protection include coadministration of basic amino acids, the bovine gelatin-containing solution Gelofusine or albumin fragments, which interfere with the tubular reabsorption pathway of peptides (for a recent review, see [21]). These and other researches have led to developments of more ideal peptide probes for tumor imaging and therapy, and the knowledge can be expanded to further modification of TK4.

Our current research showed that TK4 is homologous to a FN3 domain in a novel protein similar to vertebrate fibronectin family and that the TK4 binding on cancer cells can be inhibited by fibronectin (Figure 5), suggesting that TK4 may have targeted tumors via fibronectin-binding site(s). Fibronectin is a glycoprotein which serves as one of the major fractions of ECM. It contains an array of repeating domains (FN1, 2, and 3) that mediate interactions between cells, other ECM components (e.g., collagen), and other fibronectin molecules [15]. The tumor-targeting motif RGD, which serves as a common binding site for a variety of integrins, has been originally derived from the tenth FN3 repeat in fibronectin [15]. Besides RGD, other peptide sequences have been exploited from FN domains with cell-binding activity such as the essential $\alpha_4\beta_1$ adhesion motif LDV [23], the 25-mer endothelial cell adhesion peptide CS1 [24], and the mesenchymal stem cell-adhesive peptide ALNGR that interacts with integrin β_1 [25]. These studies would suggest that due to the pivotal role of fibronectin in the complex ECM architecture, novel binding motif residing in FN sequences or their homologous domains, like TK4, may be still discovered. We have recently found that TK4 binds efficiently to human lung cancer cell lines and that the binding can be also inhibited by fibronectin pretreatment (data not shown). Thus one of our future works will be to evaluate the potential of TK4 as a multitumor-targeting probe. Identifying the cell surface receptor(s) of TK4 on tumor cells, certainly, is crucial and should be performed in the future.

In conclusion, our data presented here showed that TK4, a novel peptide isolated from phage display library, showed a homology to FN3 domain and can target fibrosarcoma tumor cells in vivo after systemic administration. TK4 holds promise as a lead structure useful for selective delivery of therapeutics or diagnostic probe to fibrosarcoma or other tumors.

Abbreviations

BLI:	Bioluminescence imaging
ECM:	Extracellular matrix
IV:	Intravenously
FN3:	Fibronectin type III domain
FRI:	Fluorescence reflectance imaging
GRP:	Gastrin-releasing peptide
HSV1-tk:	Herpes simplex virus type 1 thymidine kinase
SPECT:	Single photon emission computed tomography
% ID/g:	Percentage of injected dose per gram.

Acknowledgments

This work is supported by the Core Facility Grant (no. 97-3112-B-010-016), National Science Council (Grant no. NSC97-2314-B-038-033-MY3). This work is also supported by the Department of Health (DOH) to Taipei Medical University—Center of Excellence for Cancer Research (TMU-CECR, DOH99-TD-C-111-008).

References

[1] M. Genoni, A. M. Biraima, B. Bode, A. C. Shah, M. B. Winkler, and M. I. Turina, "Combined resection and adjuvant therapy improves prognosis of sarcomas of the pulmonary trunk," *Journal of Cardiovascular Surgery*, vol. 42, no. 6, pp. 829–833, 2001.

[2] H. Tsuchiya, K. Tomita, Y. Mori, N. Asada, and N. Yamamoto, "Marginal excision for osteosarcoma with caffeine assisted chemotherapy," *Clinical Orthopaedics and Related Research*, no. 358, pp. 27–35, 1999.

[3] M. D. Cameron, E. E. Schmidt, N. Kerkvliet et al., "Temporal progression of metastasis in lung: cell survival, dormancy, and location dependence of metastatic inefficiency," *Cancer Research*, vol. 60, no. 9, pp. 2541–2546, 2000.

[4] J.-T. Zhang and Y. Liu, "Use of comparative proteomics to identify potential resistance mechanisms in cancer treatment," *Cancer Treatment Reviews*, vol. 33, no. 8, pp. 741–756, 2007.

[5] R. Pérez-Tomás, "Multidrug resistance: retrospect and prospects in anti-cancer drug treatment," *Current Medicinal Chemistry*, vol. 13, no. 16, pp. 1859–1876, 2006.

[6] M. Nogawa, T. Yuasa, S. Kimura et al., "Monitoring luciferase-labeled cancer cell growth and metastasis in different in vivo

models," *Cancer Letters*, vol. 217, no. 2, pp. 243–253, 2005.

[7] N. Yamamoto, M. Yang, P. Jiang et al., "Real-time GFP imaging of spontaneous HT-1080 fibrosarcoma lung metastases," *Clinical and Experimental Metastasis*, vol. 20, no. 2, pp. 181–185, 2003.

[8] D. K. Marsee, D. H. Y. Shen, L. R. MacDonald et al., "Imaging of metastatic pulmonary tumors following NIS gene transfer using single photon emission computed tomography," *Cancer Gene Therapy*, vol. 11, no. 2, pp. 121–127, 2004.

[9] W.-P. Deng, C.-C. Wu, C.-C. Lee et al., "Serial in vivo imaging of the lung metastases model and gene therapy using HSV1-tk and ganciclovir," *Journal of Nuclear Medicine*, vol. 47, no. 5, pp. 877–884, 2006.

[10] J. C. Reubi and H. R. Maecke, "Peptide-based probes for cancer imaging," *Journal of Nuclear Medicine*, vol. 49, no. 11, pp. 1735–1738, 2008.

[11] S. Zitzmann, W. Mier, A. Schad et al., "A new prostate carcinoma binding peptide (DUP-1) for tumor imaging and therapy," *Clinical Cancer Research*, vol. 11, no. 1, pp. 139–146, 2005.

[12] V. Rufini, M. L. Calcagni, and R. P. Baum, "Imaging of Neuroendocrine Tumors," *Seminars in Nuclear Medicine*, vol. 36, no. 3, pp. 228–247, 2006.

[13] R. P. J. Schroeder, W. M. V. Weerden, C. Bangma, E. P. Krenning, and M. D. Jong, "Peptide receptor imaging of prostate cancer with radiolabelled bombesin analogues," *Methods*, vol. 48, no. 2, pp. 200–204, 2009.

[14] C. Van De Wiele, P. Phonteyne, P. Pauwels et al., "Gastrin-releasing peptide receptor imaging in human breast carcinoma versus immunohistochemistry," *Journal of Nuclear Medicine*, vol. 49, no. 2, pp. 260–264, 2008.

[15] M. Leiss, K. Beckmann, A. Girós, M. Costell, and R. Fässler, "The role of integrin binding sites in fibronectin matrix assembly in vivo," *Current Opinion in Cell Biology*, vol. 20, no. 5, pp. 502–507, 2008.

[16] R. Haubner and C. Decristoforo, "Radiolabelled RGD peptides and peptidomimetics for tumour targeting," *Frontiers in Bioscience*, vol. 14, pp. 872–886, 2009.

[17] R. Brissette and N. I. Goldstein, "The use of phage display peptide libraries for basic and translational research," *Methods in Molecular Biology*, vol. 383, pp. 203–213, 2007.

[18] K. C. Brown, "Peptidic tumor targeting agents: the road from phage display peptide selections to clinical applications," *Current Pharmaceutical Design*, vol. 16, no. 9, pp. 1040–1054, 2010.

[19] W. K. Yang, L. Y. Ch'ang, C. K. Koh, F. E. Myer, and M. D. Yang, "Mouse endogenous retroviral long-terminal-repeat (LTR) elements and environmental carcinogenesis," *Progress in nucleic acid research and molecular biology*, vol. 36, pp. 247–266, 1989.

[20] R. Haubner, "$\alpha v\beta 3$-integrin imaging: a new approach to characterise angiogenesis?" *European Journal of Nuclear Medicine and Molecular Imaging*, vol. 33, no. 13, pp. S54–S63, 2006.

[21] E. J. Rolleman, M. Melis, R. Valkema, O. C. Boerman, E. P. Krenning, and M. de Jong, "Kidney protection during peptide receptor radionuclide therapy with somatostatin analogues," *European Journal of Nuclear Medicine and Molecular Imaging*, pp. 1–14, 2009.

[22] T. M. Behr, D. M. Goldenberg, and W. Becker, "Reducing the renal uptake of radiolabeled antibody fragments and peptides for diagnosis and therapy: present status, future prospects and limitations," *European Journal of Nuclear Medicine*, vol. 25, no. 2, pp. 201–212, 1998.

[23] A. Komoriya, L. J. Green, M. Mervic, S. S. Yamada, K. M. Yamada, and M. J. Humphries, "The minimal essential sequence for a major cell type-specific adhesion site (CS1) within the alternatively spliced type III connecting segment domain of fibronectin is leucine-aspartic acid-valine," *Journal of Biological Chemistry*, vol. 266, no. 23, pp. 15075–15079, 1991.

[24] E. J. Rodenberg and F. M. Pavalko, "Peptides derived from fibronectin type III connecting segments promote endothelial cell adhesion but not platelet adhesion: implications in tissue-engineered vascular grafts," *Tissue Engineering*, vol. 13, no. 11, pp. 2653–2666, 2007.

[25] M. Okochi, S. Nomura, C. Kaga, and H. Honda, "Peptide array-based screening of human mesenchymal stem cell-adhesive peptides derived from fibronectin type III domain," *Biochemical and Biophysical Research Communications*, vol. 371, no. 1, pp. 85–89, 2008.